Journal of Catalysis **205,** 58–66 (2002)
doi:10.1006/jcat.2001.3421, available online at http://www.idealibrary.com on IDEAL®

Effect of Treatment with $NaAlO_2$ Solution on the Surface Acid Properties of Zeolite β

Xie Zaiku,*,†,[1] Bao Jiaqing,* Yang Yiqing,* Chen Qingling,* and Zhang Chengfang†

*Shanghai Research Institute of Petrochemical Technology, Shanghai 201208, People's Republic of China; and †Institute of Chemical Technology, East China University of Science and Technology, Shanghai 200237, People's Republic of China

Received April 24, 2001; revised July 19, 2001; accepted August 30, 2001

The influence of treatment with an $NaAlO_2$ aqueous solution of $NaAlO_2$ on the surface acid properties of zeolite β was studied as a method to increase the number of both Brønsted and Lewis acid sites. The Hβ samples, prepared by treating with an aqueous solution of $NaAlO_2$, were characterized by XRD, NH_3-TPD, pyridine-IR, ^{29}Si MAS NMR, and ^{27}Al MAS NMR. The surface properties of the Hβ zeolite changed after treatment with the aqueous $NaAlO_2$ solution: the number of strong and weak acid sites, the total amount of acid, and the Brønsted and Lewis acid sites increased. The treatment of zeolite β with an aqueous solution of $NaAlO_2$ may realuminate an $Si(0Al)_A$ site by the isomorphous substitution of $Al(OH)_4^-$ anions. © 2002 Elsevier Science

Key Words: **zeolite β; acid sites; dealumination; realumination; $NaAlO_2$ treatment.**

INTRODUCTION

The acidic properties of zeolites are closely linked to the quantity, nature, and distribution of the aluminum atoms that are attached to or trapped in the three-dimensional network of pores and cavities. The outstanding catalytic activity of zeolites is due to their pore structure and to the acid sites on the surface. Hence, controlling the acidity of a zeolite is one of the most important topics in the study of zeolite catalysis. The acid sites in zeolites are linked to the tetrahedral aluminum atoms in the framework of the zeolite. Therefore, the acidity depends on the amount of framework aluminum. However, it is not easy to widely vary the content of framework aluminum in all zeolites during the process of hydrothermal synthesis.

Postsynthetic methods, such as dealumination and realumination, are often more practicable and useful for varying the Al content. The dealumination/realumination process can be regarded as an isomorphous substitution of the type $[Si^{4+}, Al^{3+}]_F \longleftrightarrow [Si^{4+}]_F + [Al^{3+}]_{EF}$, where the subscripts F and EF denote framework and extra-framework atoms, respectively. The dealumination process has been studied extensively (1). Dealumination by thermal, hydrothermal, or mineral acid treatments is well-known and used widely for Y, ZSM-5, β, and mordenite zeolites (2). However, the reverse process, whereby extra-framework aluminum is reinserted into the tetrahedral framework, has been described only recently in a small number of papers (3–8). Most of the work has dealt with Y, ZSM-5, and mordenite. For example, it was reported that the extra-framework aluminum produced by hydrothermal treatment can be subsequently reinserted into the framework of Y (9) and ZSM-5 (10) by treatment with an aqueous solution of KOH, NaOH, or NH_3 at elevated temperature. On the other hand, a treatment with $AlCl_3$ vapor at elevated temperature was said to incorporate Al atoms into the framework of highly siliceous ZSM-5 zeolite and, thus, change its acidity and activity (4, 5, 11, 12). A similar technique using other metal chlorides successfully incorporated Ga, Sb, As, In, and B atoms into the ZSM-5 framework to prepare metallosilicates of various acid strengths. Third, a treatment with an aqueous solution of $NaAlO_2$ was also reported to incorporate Al atoms into the framework of Y (13), but the influence of the $NaAlO_2$ solution treatment on surface acid properties has not been discussed.

Zeolite β is a Mobil proprietary material first synthesized in 1967 by Wadlinger *et al.* (14). The structure of zeolite β was described by Treacy and Newsam (15). Due to its special pore system and surface acidity, zeolite β is a candidate for use as a solid acid catalyst. The catalytic properties of zeolite β in the cracking of paraffins (16), in the isomerization of *n*-heptane (17) and *n*-hexane (18), and in the disproportionation and transalkylation of toluene and C_9 aromatics (19, 20) were recently reported.

Of the many publications on the acidity of zeolite β, the following points are of special importance: (i) Among the ion-exchanged forms of zeolite β, Hβ zeolite possesses the highest acidity (21). (ii) Any treatment that affects the coordination state of aluminum results in a change in the number and types of acid sites (22, 23). The total acidity of zeolite β depends strongly on the type of ion exchange and the acid treatment. Zeolite β has been ion-exchanged with solutions of ammonium acetate (24), ammonium nitrate

[1] To whom correspondence should be addressed. Fax: 86-21-6846-2283. E-mail: xzk@sript.com.cn.

0021-9517/02 $35.00

(25–27), and ammonium chloride (28, 29), and zeolite β has been treated with inorganic (24, 27, 30, 31) and organic acids (32). It was recently reported by Yang and Xu (31) that a realuminated zeolite β was obtained by treating dealuminated zeolite β with an aqueous $NaAlO_2$ solution. Yang and Xu studied factors such as the content, temperature, and pH of the $NaAlO_2$ solution on the basis of the characterization of aluminated samples by XRD and FTIR. The distribution of Al and Si in zeolite β, the surface acid properties, and the realuminum mechanism were not studied, however.

In the present work, zeolite β, synthesized by using tetraethylammonium (TEA) hydroxide as an organic template, and sodium aluminate as the aluminum source was ion-exchanged by ammonium nitrate solution and then treated with an $NaAlO_2$ solution. The surface acid properties of the Hβ, obtained by high-temperature calcination of $NH_4\beta$, and the process of realumination over Hβ were explored. In addition, the catalytic activity of zeolite β for toluene disproportionation and C_9 aromatics transalkylation, before and after treatment with the $NaAlO_2$ solution were compared.

EXPERIMENTAL

Preparation of Hβ

Zeolite β was synthesized at 150 to 170°C for 60 h using a hydrothermal method (32); silica gel was used as the silica source; sodium aluminate was used as the aluminum source; and tetraethylammonium (TEA) hydroxide was used as the template with a reaction of the following composition: $2.36Na_2O \cdot Al_2O_3 \cdot 2.2(TEA)_2O \cdot 40SiO_2 \cdot 108H_2O$. The as-synthesized sample (TEAβ) was calcined at 550°C for 5 h in an air stream and ion-exchanged four times with a 10 wt% ammonium nitrate solution for 4 h at 80 to 90°C. The $NH_4\beta$ sample was then calcined for 5 h at 550°C in an air stream (giving the sample Hβ(0), with a chemical molar Si/Al ratio of 19) and then treated with a 0.03 M (pH = 12.6) and 0.33 M (pH = 13.4) $NaAlO_2$ solution for 4 h at 80 to 90°C, respectively. The two aluminated samples were then dried in air for 5 h at 120°C and then calcined in an air stream for 5 h at 550°C, to give samples Hβ(0.03) and Hβ(0.33) with chemical molar Si/Al ratios of 16.5 and 14.3, respectively.

Characterization

XRD determinations were carried out on a Rigaku D/max-1400-ray diffractometer at 40 kV with 40 mA and Cu$K\alpha$ radiation; the samples were saturated with $CaCl_2$ before the test.

A self-supported wafer of about 10 mg with a diameter of 15 mm was placed in an infrared quartz cell with CaF_2 windows and connected to a vacuum system. The wafer was dehydrated at 400°C at $P = 10^{-5}$ Torr for 6 h. The background spectra of the samples were recorded after the self-supported wafer was cooled to ambient temperature and pyridine vapors were admitted to the cell. The temperature of the sample was increased to 120°C, and the pyridine vapor was adsorbed for 5 min. Finally, excess of pyridine was desorbed by evacuating the samples at the desired temperature (namely, 120, 180, 240, and 300°C) for 0.5 h. The samples were cooled to ambient temperature, and the spectra were recorded on a Bruker IFS 88 spectrometer with a resolution of 4.0 cm^{-1}.

TPD of NH_3 was carried out on a Zeton Altamira AMI-100 apparatus. The NH_3 was adsorbed at 120°C. The Hβ sample was measured at a heating rate of 10°C min^{-1}. Helium was used as the carrier gas with a flow rate of 40 mL min^{-1}.

Solid-state MAS NMR spectra were measured on a Bruker AMX-400 spectrometer via single-pulse experiments at a spinning rate of around 4 kHz. ^{29}Si MAS NMR spectra were recorded at 79.49 MHz with a pulse width of 2 μs (45°), and a time interval between pulse sequences of 4 s. Chemical shifts were referenced to external TMS. ^{27}Al MAS NMR spectra were recorded at 104.26 MHz using a short pulse width of 0.5 μs ($<\pi/12$) to ensure quantitative line intensities; the time interval between pulse sequences was 1 s. Chemical shifts were referenced to external $Al(H_2O)_6^{3+}$ in $AlCl_3$ aqueous solution. All the samples were equilibrated with the saturated water vapor of an NH_4Cl solution before packing into the NMR MAS rotors.

Catalytic Activity

The catalytic activity of Hβ determined by means of the reaction of toluene disproportionation and C_9 aromatics transalkylation in a continuous fixed-bed micro reactor. A mixture of 2.0 g of 20- to 30-mesh zeolite and 2 g of glass chips were packed into the reactor and activated at the desired reaction temperature (385°C) in hydrogen gas at a pressure of 2.8 MPa for 2 h. A mixture of toluene (Yangzi Petrochemical Corp.) and C_9 aromatics (Yangzi Petrochemical Corp.) with a weight ratio of 1 : 1 and at a weight hourly space velocity (WHSV) of 2.5 h^{-1} was then conducted into the reactor by a metering pump; the hydrogen gas with a molar ratio of hydrogen to mixture of toluene and C_9 aromatics of 4 : 1 was also introduced into the reactor. The reaction products were collected and analyzed with an HP5890 II gas chromatograph equipped with a capillary column of PEG 20 M * 0.25 mm * 50 m.

The conversions, either the disproportionation or transalkylation of toluene, X_T, and of C_9 aromatics, X_{C_9}, and of all aromatics, X, and the selectivity of benzene and xylene (B + X), $S_{(B+X)}$, are defined, respectively, as

$$X_T = \frac{(\text{toluene mol\%})_F - (\text{toluene mol\%})_P}{(\text{toluene mol\%})_F}$$

$$X_{C_9} = \frac{(C_9\ \text{mol\%})_F - (C_9\ \text{mol\%})_P}{(C_9\ \text{mol\%})_F}$$

$$X = \frac{(\text{toluene mol\%} + C_9\ \text{mol\%})_F - (\text{toluene mol\%} + C_9\ \text{mol\%})_P}{(\text{toluene mol\%} + C_9\ \text{mol\%})_F}$$

$$S_{(B+X)} = \frac{(\text{benzene mol\%} + \text{xylene mol\%})_P - (\text{benzene mol\%} + \text{xylene mol\%})_F}{(\text{toluene mol\%} + C_9\ \text{mol\%})_F - (\text{toluene mol\%} + C_9\ \text{mol\%})_P},$$

where the subscripts F and P represent the component in the feed stream and in the product stream, respectively.

RESULTS AND DISCUSSION

XRD Study

Figure 1 shows the XRD patterns, recorded before and after the $NaAlO_2$ treatment. The $NaAlO_2$ treatment product is pure zeolite β, and the structure of the zeolite β is essentially retained. Moreover, the intensity of the XRD peaks did not change after the treatment with a 0.03 M $NaAlO_2$ solution, which indicates that the aluminated sample still possesses high relative crystallinity. When zeolite β was treated with a 0.33 M $NaAlO_2$ solution with a higher alkalinity, the relative crystallinity of the aluminated sample decreased to 53%, and the width in the middle of the aluminated sample was larger than that of the sample that was not aluminated. Consequently, the crystal size of the aluminated sample is smaller. These facts suggest that destruction of the framework of the samples takes place due to the dissolution of a number of silicon atoms of the framework in the highly alkaline (pH > 13) solution. Therefore, we conclude that the alkalinity of the solution used for the aluminated sample should not be too high, i.e., pH < 13, different from the pH used in the alumination of zeolite Y (13).

NH_3-TPD Study

Table 1 lists the results of the NH_3-TPD of all the samples, before and after the $NaAlO_2$ treatment. The results indicate that, when the Naβ sample is ion-exchanged by ammonium nitrate, calcined at 550°C, and then treated with an $NaAlO_2$ solution, there is an increase in the amount of weak, strong, and total acid on the surface of Hβ zeolite. This is similar to our previous results of a study of zeolite β after treatment with citric acid (32).

TABLE 1

NH_3-TPD Data of the Hβ Samples

Sample[a]	T peak/°C		n_{NH_3}/mmol g^{-1}		
	LT[b] peak	HT[c] peak	Total acid amount[d]	Weak acid amount[d]	Strong acid amount[d]
Hβ(0)	250	425	0.36	0.30	0.06
Hβ(0.03)	230	415	1.55	0.55	1.00

[a] Content of $NaAlO_2$ shown in parentheses.
[b] Low-temperature peak.
[c] High-temperature peak.
[d] The experimental error is less than 5% of each value.

Infrared Spectroscopy Study

Figures 2 and 3 present the IR spectra of pyridine adsorbed on the zeolite in the 1600- to 1370-cm^{-1} region. There are three sharp bands due to C–C stretching vibrations of pyridine. The strong band at 1489 cm^{-1} is due to the pyridine adsorbed on both Brønsted and Lewis acid sites, while the bands at 1542 and 1453 cm^{-1} are due to protonation of the pyridine molecule by Brønsted acid sites and to pyridine adsorbed on Lewis acid sites, respectively. The relative concentration of Brønsted and Lewis acid sites was determined using the relation $B/L = (A_B/A_L)(\varepsilon_L/\varepsilon_B)$, where A_B/A_L is the absorbance ratio and $\varepsilon_L/\varepsilon_B$ the extinction coefficient ratio. The $\varepsilon_L/\varepsilon_B$ value is 0.546 for β zeolites (33).

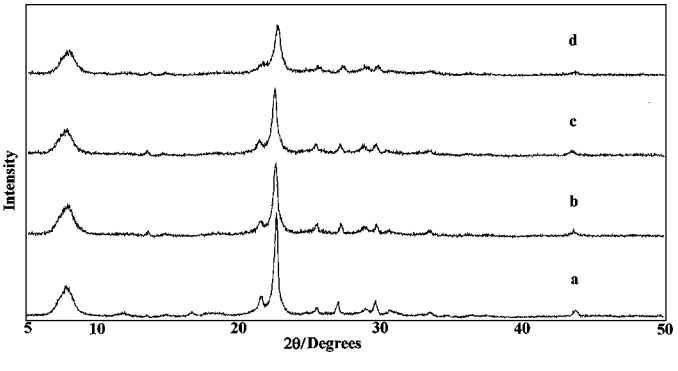

FIG. 1. XRD patterns before and after $NaAlO_2$ treatment for zeolite β: (a) TEAβ, (b) Hβ(0), (c) Hβ(0.03), (d) Hβ(0.33).

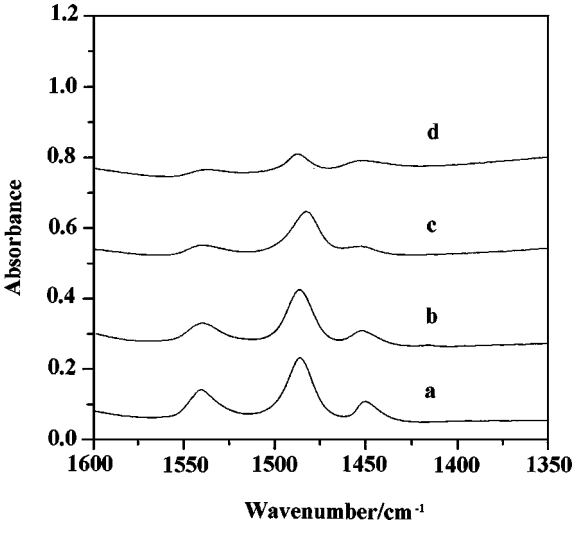

FIG. 2. IR spectra of pyridine on Hβ(0) at different pyridine desorption temperatures: (a) 120°C, (b) 180°C, (c) 240°C, (d) 300°C.

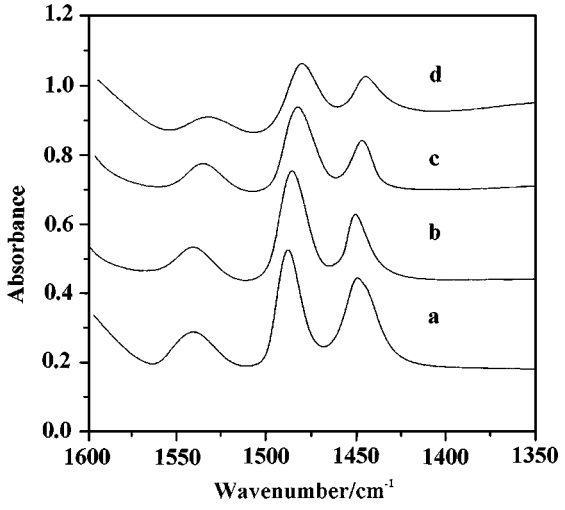

FIG. 3. IR spectra of pyridine on Hβ(0.03) at different pyridine desorption temperatures: (a) 120°C, (b) 180°C, (c) 240°C, (d) 300°C.

Table 2 lists the Brønsted acid sites, the Lewis acid sites, and the B/L ratios for pyridine desorption at different temperatures.

Table 2 shows that the Brønsted and Lewis acid sites of Hβ(0) and Hβ(0.03) differ at pyridine desorption temperatures of 120 to 300°C. The number of Brønsted acid sites of Hβ(0.03) is larger than that of Hβ(0), as is the number of Lewis acid sites. This indicates that the number of Brønsted and Lewis acid sites increased as a result of the $NaAlO_2$ solution treatment. These results are similar to those of our previous study (32), in which the number of Brønsted and Lewis acid sites of Hβ zeolite increased when Hβ zeolite was treated with citric acid.

Figures 2 and 3 show the effect of desorption temperature on the relative intensity of the pyridine Brønsted and Lewis acid bands of the Hβ(0) and Hβ(0.03) samples. It is obvious that the relative intensity of the Brønsted acid band gradually decreased with increasing desorption temperature, and that the intensity of the Lewis acid band also decreased with increasing desorption temperature of the Hβ(0) and Hβ(0.03) samples; however, the B/L ratios of Hβ(0) gradually decreased and those of Hβ(0.03) gradually increased with increasing pyridine desorption temperature (see Table 2). It is concluded that the strength of the Brønsted site is weaker than that of the Lewis acid sites for Hβ(0), and that the strength of the Brønsted site is stronger than that of the Lewis acid sites for Hβ(0.03).

^{29}Si MAS NMR, ^{27}Al MAS NMR Spectroscopy

In order to explain the change in the type and amount of acid in the zeolite β treated with an $NaAlO_2$ solution, the TEAβ, Hβ(0), and Hβ(0.03) samples were characterized by ^{29}Si and ^{27}Al MAS NMR. Tables 3 and 4 give the NMR results of silicon and aluminum for the TEAβ, Hβ(0), and Hβ(0.03) samples.

The Si/Al ratio in the framework is calculated by deconvoluting the ^{29}Si MAS NMR spectra. Using Gaussian line shapes, four lines of the Si(nAl) ($n = 0, 1, 2, 3$) sites and one line of the Si(O^-) site were deconvoluted from the spectra of Hβ zeolite (34). The framework Si/Al ratio of TEAβ, Hβ(0), and Hβ(0.03) was determined according to (34, 35)

$$\left(\mathrm{Si}/\mathrm{Al}\right)_{\mathrm{NMR}} = \frac{\sum_{n=0}^{2} I_{\mathrm{Si}(n\mathrm{Al})}}{\sum_{n=0}^{2} \frac{n}{4} \cdot I_{\mathrm{Si}(n\mathrm{Al})}},$$

where $I_{\mathrm{Si}(n\mathrm{Al})}$ is the intensity or the population of a ^{29}Si MAS NMR peak. Figure 4 shows the experimental ^{29}Si MAS NMR spectra and the deconvoluted ^{29}Si MAS NMR spectra using Gaussian line shapes of TEAβ, Hβ(0), and Hβ(0.03).

In the TEAβ, Hβ(0), and Hβ(0.03) samples, two lines centered at around −114 and −110 ppm were ascribed to Si(0Al) of two different crystallographic sites (29, 34, 36), $Si(0Al)_A$ and $Si(0Al)_B$. According to the coordination sequences of T-atoms in the zeolite β structure (37), the ^{29}Si MAS NMR spectrum of zeolite β should have nine lines.

TABLE 2

Comparison of Acid Sites and B/L Ratios as Seen in the Pyridine-IR Spectra of the Hβ Samples[a]

	Temperature/°C ($\times 10^{20}$sites/g)											
	120			180			240			300		
Sample	B acid sites[b]	L acid sites[b]	B/L[c]	B acid sites[b]	L acid sites[b]	B/L[c]	B acid sites[b]	L acid sites[b]	B/L[c]	B acid sites[b]	L acid sites[b]	B/L[c]
Hβ(0)	1.09	0.57	1.05	0.99	0.51	1.05	0.42	0.42	0.55	0.17	0.32	0.29
Hβ(0.03)	1.66	1.63	0.55	1.62	1.01	0.87	1.43	0.80	0.98	1.39	0.72	1.05

[a] The experimental error is less than 5% of each value.
[b] Calculated from the ratio of the integrated area of the IR adsorption peak to sample weight.
[c] Calculated according to the equation $0.546 \times (A_B/A_L)$, where A_B/A_L is the absorbance ratio.

TABLE 3

^{29}Si MAS NMR Data for TEAβ and Hβ Samples

		$Si(0Al)_A$ site			$Si(0Al)_B$ site			Si(1Al) site			$Si(O^-)$ site			Si(2Al) site		
Sample[a]	Si/Al[b]	CS[c]	LW[d]	P[e]	CS	LW	P	CS	LW	P	CS	LW	P	CS	LW	P
TEAβ	12.7	114.4	1.86	20.0	110.7	1.86	45.6	107.2	2.14	13.7	103.6	2.03	13.2	100.5	3.02	7.6
Hβ(0)	21.1	113.9	1.79	23.3	110.5	1.79	47.7	105.5	2.17	14.4	102.4	2.24	13.6	99.1	1.22	1.0
Hβ(0.03)	17.7	114.2	1.67	18.6	110.7	1.92	50.4	105.5	2.55	15.7	102.3	2.40	13.3	98.1	1.74	2.0

[a] The content of $NaAlO_2$ are in parentheses.
[b] The experimental error is less than 0.2 (35).
[c] Chemical shift assignment from Refs. 38, 45, and 46.
[d] Line width.
[e] Relative population of Si(nAl) tetrahedral building blocks in the samples (normalized to 100), calculated according to Gaussian deconvolution of ^{29}Si MAS NMR spectra.

Fyfe *et al.* (36) showed that the ^{29}Si MAS NMR spectrum of highly dealuminated zeolite β has three groups of nine peaks centered at −115, −113, and −111 ppm for each group. Perez-Pariente *et al.* (29) showed only three lines for calcined zeolite β. Chao *et al.* (34) showed that the ^{29}Si MAS NMR spectrum of zeolite β has two lines centered at around −114−−115 and −110 ppm. These different results may be caused by the low resolution in the ^{29}Si MAS NMR spectra due to the higher concentration of the stacking in zeolite β (29). Figure 4 and Table 3 show that Si(1Al), Si(O^-), and Si(2Al) sites are centered at −107−−105, −103−−102, and −100−−99 ppm, respectively (29, 38).

The experimental ^{27}Al MAS NMR spectra and the ^{27}Al MAS NMR spectra deconvoluted by using Gaussian line shapes of TEAβ, Hβ(0), and Hβ(0.03) are shown in Fig. 5. Although the presence of second-order quadrupolar effects seems to decrease the ^{27}Al MAS NMR spectral resolution, it is obsverved that there are two peaks centered at 51 to 54 and 55 to 58 ppm, assigned to framework tetrahedral aluminum (T_dAl), as found in previous studies (29, 32). van Bokhoven *et al.* (39) proved the presence of two different tetrahedral aluminum species in β zeolites by using a MQ MAS NMR. T_dAl may have two different crystallographic

TABLE 4

^{27}Al MAS NMR Data for TEAβ and Hβ Samples[a]

	Chemical shift[b]			Al content[c]/%			
Sample	T_dAl of site A	T_dAl of site B	O_hAl	T_dAl of site A	T_dAl of site B	I_A/I_B[d]	O_hAl
TEAβ	51.4	54.8	/	43.1	56.9	0.76	0
Hβ(0)	54.2	57.9	2	50.0	40.4	1.24	9.6
Hβ(0.03)	54.0	57.7	2	56.5	36.1	1.56	7.4

[a] The experimental error is less than 0.1(35).
[b] Chemical shift assignment from Refs. 38, 45, and 46.
[c] Relative amounts of tetrahedral and octahedral aluminum.
[d] $I_A/I_B = T_d$Al of site A/T_dAl of site B.

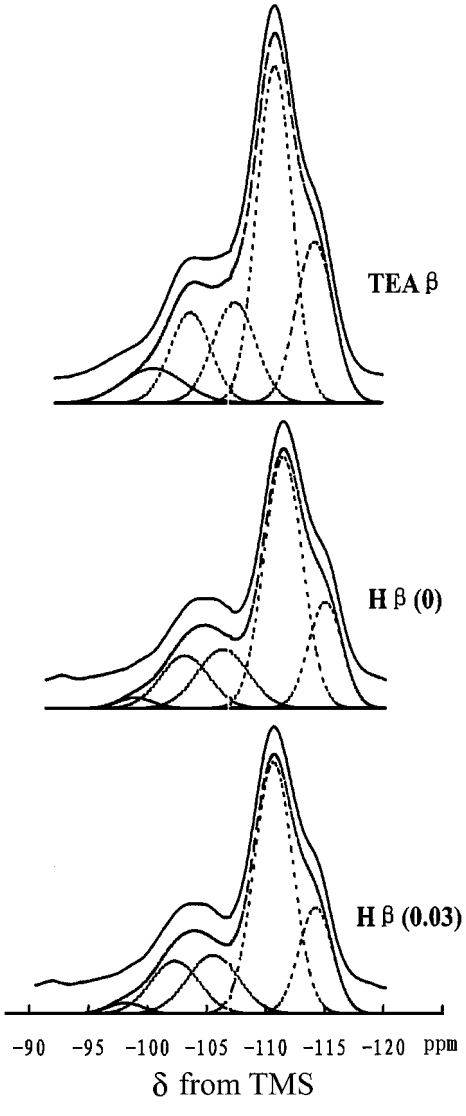

FIG. 4. Experimental and deconvoluted ^{29}Si MAS NMR spectra of TEAβ, Hβ(0), and Hβ(0.03). Top, experimental spectrum; middle, simulated spectrum; bottom, deconvoluted spectrum.

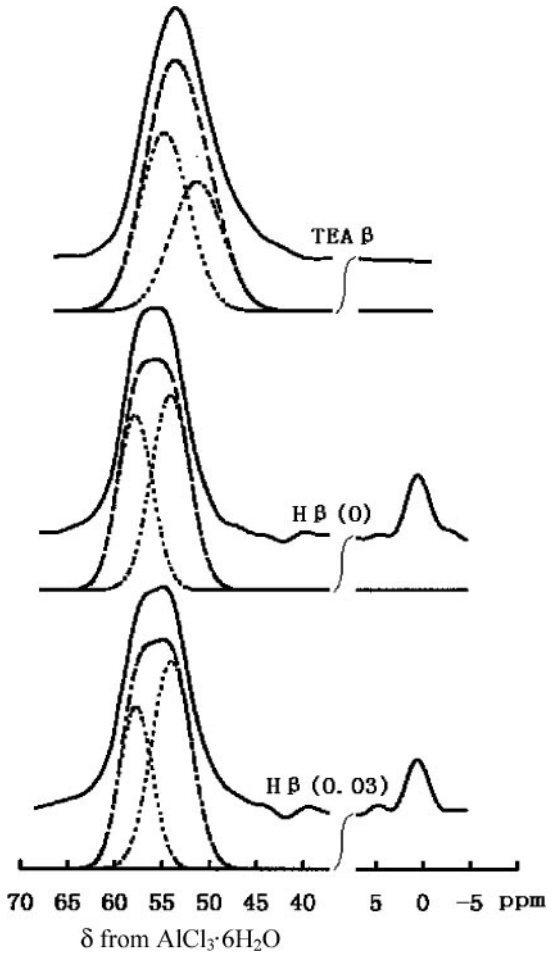

FIG. 5. Experimental and deconvoluted ^{27}Al MAS NMR spectra of TEAβ, Hβ(0), and Hβ(0.03). Top, experimental spectrum; middle, simulated spectrum; bottom, deconvoluted spectrum.

sites in the framework of Hβ zeolite. The first, site A, is located in the four-membered rings of the framework (S4R). The second, site B, is located in the six-membered rings of the framework (S6R). Chauvin and co-workers (35, 40) and Klinowski and Anderson (41) found similar results for Ω zeolite, which has six- and four-membered rings. In addition, a line centered at 1 ppm was also observed, corresponding to nonframework aluminum (O_hAl).

After the TEAβ sample was calcined and ion-exchanged and the $NH_4\beta(0)$ sample was calcined to make the sample Hβ(0), several changes were observed in the spectra (Tables 3 and 4). The framework Si/Al ratios increased considerately; i.e., the framework Al content decreased, the total number of Si(0Al) and Si(1Al) sites increased from 65 to 71 and 13.7 to 14.4, respectively, and the Si(2Al) sites remarkably decreased from 7.6 to 1. Site B of T_dAl decreased strongly from 56.9 to 40.4%, and site A of T_dAl increased strongly from 43.1 to 50.0%, while the corresponding I_{siteA}/I_{siteB} ratio increased from 0.76 to 1.24. These observations are also supported by the increase in the O_hAl/T_dAl ratio, which indicates that zeolite β becomes dealuminated mainly by deep-bed calcination. The dealumination of zeolite β, which was studied in the presence of a dilute acid solution, has been attributed (42) to the location of the aluminum atoms in the center of S-shaped chains of five tetratomic rings. Such a strained structure would be chemically and thermally unstable. During the process of thermal dealumination of the zeolite, the aluminum is not removed equally from the different sites; those corresponding to the 53 to 54 ppm resonance signal are more resistant to dealumination than those associated with the 57 ppm line; i.e., site B can be dealuminated more easily than site A. The analysis indicates that the TEAβ was dealuminated during calcination, and that there are Si(1Al) and Si(2Al) sites in the TEAβ However, one question remains: which aluminum atoms of the Si(1Al) and Si(2Al) sites or which T_dAl of sites A and B are removed from the zeolite β framework? The experiments show that the Si(2Al) sites decrease remarkably from 7.6 to 1, and the I_{siteA}/I_{siteB} ratio increases from 0.76 to 1.24. As a result, the dealumination of TEAβ during calcination may take place at a Si(2Al) site shown in the ^{29}Si MAS NMR spectra and at a T_dAl of site B shown in the ^{27}Al MAS NMR spectra.

Comparing Hβ(0) and Hβ(0.03), the framework Si/Al ratio decreases from 21.1 to 17.7; i.e., the content of Al in the framework increases (see Table 3). This indicates that zeolite β is realuminated during the treatment with $NaAlO_2$ solution. Table 3 shows that there is a decrease in the relative population of the $Si(0Al)_A$ sites and an increase in the relative population of the Si(1Al) and Si(2Al) sites. Table 4 shows an increase in framework aluminum, a decrease in the relative amount of octahedral aluminum, a decrease in site B of T_dAl, an increase in site A of T_dAl, and a corresponding increase in the I_{siteA}/I_{siteB} ratio from 0.76 to 1.24. These changes indicate that Hβ was probably realuminated at the $Si(0Al)_A$ site during the $NaAlO_2$ solution treatment.

The acidity usually depends on the aluminum content and the strength of the acid sites of the zeolite (43). We are of the opinion that the surface acidity of the Hβ(0) and Hβ(0.03) samples is not only related to the framework Si/Al ratio of Hβ zeolite but is also effected by the coordination and distribution of framework silicon and aluminum sites. van Hooff (44) reached a similar conclusion after studying HZSM-5 zeolite with a framework Si/Al ratio of 9 to 10. Previous studies (10, 11, 47, 48) indicate that framework silicon and aluminum sites and their distribution changed during dealumination and realumination and led to changes in the acidity of the zeolites. Furthermore, for mazzite and Y zeolite, the acidity of the framework Si(2Al) site is different from the acidity of the framework Si(1Al) site according to Guisnet *et al.* (49) and Sulikowski *et al.* (2), respectively. Table 3 shows that the number of framework

Si(2Al) sites, corresponding to less acidic $(SiO)_2(AlO)Si–OH–Al(OSi)_3$ of Hβ(0.03), is larger than that of Hβ(0); and that the number of framework Si(1Al) sites, corresponding to more acidic $(SiO)_3Si–OH–Al(OSi)_3$ of Hβ(0.03), is larger than that of Hβ(0). The Si–OH–Al group of Hβ zeolite corresponds to the Brønsted acid site. Thus, the amount of Brønsted acid in Hβ(0.03) is greater than that in Hβ(0).

Hβ Catalytic Activity of Disproportionation and Transalkylation of Toluene and C_9 Aromatics

The catalytic activity of Hβ was evaluated using toluene disproportionation and C_9 aromatics transalkylation as model reactions in a continuous fixed-bed micro reactor. The commercial C_9 aromatics used in this study were composed of 1,3,5-, 1,2,4-, 1,2,3-trimethylbenzene, *o*-ethyl toluene, *m*-ethyl toluene, *p*-ethyl toluene, and propyl benzene. The complex reactions of toluene disproportionation and C_9 aromatics transalkylation include four kinds of main reactions: disproportionation, dealkylation, transalkylation, and isomerization. The reaction scheme for toluene and C_9 aromatics conversion over β zeolite is proposed(19), for example,

(1) Disproportionation reactions:

$$2C_6H_5–CH_3 \rightleftharpoons C_6H_6 + CH_3–C_6H_4–CH_3$$

$$CH_3–C_6H_3(CH_3)–CH_3 \rightleftharpoons CH_3–C_6H_4–CH_3 + CH_3–C_6H_2(CH_3)_2–CH$$

(2) Dealkylation:

$$CH_3–C_6H_4–C_2H_5 \rightleftharpoons C_2H_4 + C_6H_5–CH$$
$$C_6H_5–C_3H_7 \rightleftharpoons C_3H_6 + C_6H_6$$

(3) Transalkylation:

$$C_6H_5–CH_3 + CH_3–C_6H_3(CH_3)–CH_3 \rightleftharpoons 2CH_3–C_6H_4–CH_3$$

(4) Isomerization:

$$1,3,5–C_6H_3(CH_3)_3 \rightleftharpoons 1,2,3–C_6H_3(CH_3)_3 \rightleftharpoons 1,2,4–C_6H_3(CH_3)_3$$

$$1,2–CH_3–C_6H_4–C_2H_5 \rightleftharpoons 1,3–CH_3–C_6H_4–C_2H_5 \rightleftharpoons 1,4–CH_3–C_6H_4–C_2H_5$$

TABLE 5

Comparison of the Activity for Disproportionation and Transalkylation of Toluene and C_9 Aromatics over Hβ(0) and Hβ(0.03)

Sample	WHSV (h^{-1})	H/C (mol)	Reaction temp. (°C)	X_T (mol%)	X_{C_9} (mol%)	X (mol%)	$S_{(B+X)}$ (mol%)
Hβ(0)	2.5	4.0	385	36.28	53.71	43.58	88.26
Hβ(0.03)	2.5	4.0	385	36.02	61.34	46.63	93.30

Table 5 gives the catalytic activity of Hβ(0) and Hβ(0.03) for disproportionation and transalkylation of toluene and C_9 aromatics. Under the experimental conditions, the catalytic activity of C_9 aromatics conversion and (B + X) selectivity of Hβ(0.03) is higher than that of Hβ(0). This indicates that the catalytic activity of zeolite β increased as a result of the $NaAlO_2$ solution treatment due to a change in the surface acid properties.

In the past (50, 51), researchers suggested that the Lewis acid site is the active site of aromatics disproportionation, and the Brønsted acid site is the active site of aromatics tran-salkylation. In the work described here, the strength of the Brønsted site is weaker than that of the Lewis acid sites for Hβ(0), and the strength of the Brønsted site is stronger than that of the Lewis acid sites for Hβ(0.03). Thus, the toluene disproportionation reactions and all three trimethylbenzene disproportionation reactions of Hβ(0.03) are weaker than those of Hβ(0), the formed C_{10} aromatics decrease; the toluene and C_9 aromatics transalkylation of Hβ(0.03) is stronger than that of Hβ(0), and the formed xylene increases. In addition, the ethyl toluene dealkylation reaction of Hβ(0.03) is stronger than that of Hβ(0) due to the increase in the amount of surface acid. As a result, the conversion of C_9 aromatics and (B + X) selectivity of Hβ(0.03) are higher than those of Hβ(0); the catalytic activity of zeolite β is improved by the $NaAlO_2$ solution treatment.

Mechanism of Realumination

Treatment of zeolite β with an aqueous solution of KOH or NaOH causes realumination (48), as does treatment with an $NaAlO_2$ solution. Many researchers presented two different realumination mechanisms for Y, ZSM-5, mordenite, and zeolite β. The first is the mechanism of isomorphous substitution of Al atoms for the framework silicon atoms (10, 11, 13, 48), i.e., the incorporation of AlO_4^- into the framework Si(0Al) site by treatment with an aqueous solution of KOH or NaOH at elevated temperature. The second mechanism is a reaction of aluminum halides with intracrystalline defective sites, such as "hydroxyl nests," by treatment with an acid solution of $AlCl_3$ (12, 13, 52, 53). Which of the mechanisms mentioned previously explains the realumination of zeolite β during the $NaAlO_2$ solution treatment? Considering the base properties of the

realumination solution, the mechanism should be similar to that of isomorphous substitution of Al atoms for the framework silicon atoms. On the other hand, the experimental results indicate that the number of framework Si(0Al) sites of Hβ(0.03) is lower than that of Hβ(0), and that the number of framework Si(0^-) sites of Hβ(0) does not change after treatment of Hβ(0) with the $NaAlO_2$ solution to prepare Hβ(0.03). The Al species are probably incorporated into the framework Si(0Al) sites, as reported by Yang and Xu (31, 54): the aluminum species were inserted into the framework both by filling the structural vacancies and by substituting the framework silicon atoms. Therefore, isomorphous substitution is probably the mechanism of realumination of zeolite β when zeolite β is treated with an $NaAlO_2$ solution. The Al atoms inserted into the zeolite originate from the nonframework Al atoms of zeolite β and of the $NaAlO_2$ solution. As previously mentioned, we describe the process of alumination of zeolite β as follows: The parent zeolite β, which is obtained by calcining the NH_4 β sample and which contains nonframework aluminum species and aluminum cations (see step 1), is aluminated in the alkaline $NaAlO_2$ solution. The aluminum species dissolve into the solution and are hydrolyzed to produce $Al(OH)_4^-$ anions (see step 2). Thus, $Al(OH)_4^-$ can be reinserted into the framework of zeolite β, and an isomorphous substitution of $Al(OH)_4^-$ anions for the framework Si(0Al) sites should occur (see step 3). The process of realumination can be described as

Step 1:

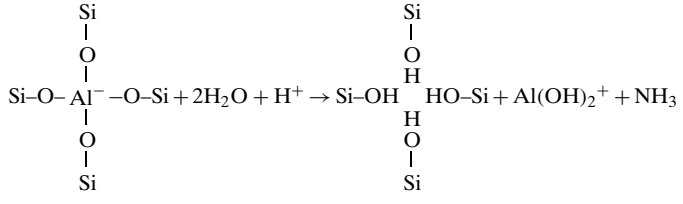

Step 2:

$$Al(OH)_2^+ + 2OH^- \rightleftharpoons Al(OH)_4^-$$

Step 3:

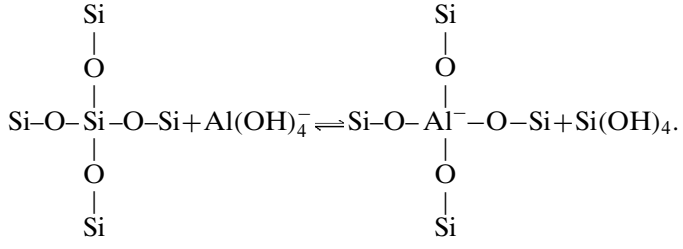

Due to the reinsertion of the extra-framework aluminum, the relative population of the Si(0Al) sites of Hβ(0.03) is smaller than that of Hβ(0), and the relative population of the Si(1Al) sites of Hβ(0.03) is larger than that of Hβ(0) (Table 3). These results indicate that realumination can occur only on the Si(0Al) site of zeolite β, i.e., on the Si(4Si) sites, and generates new Si(1Al) and Si(2Al) sites in the framework of zeolite β, thus leading to an increase in the number of Brønsted acid sites. The previous analysis is consistent with the Loewenstein rule (55). The central silicon atom can be isomorphously substituted by aluminum only according to the Loewenstein rule, which prohibits Al–O–Al linkages and is the case in all hydrothermally synthesized zeolites. According to the loop configuration for the zeolite β structure (37), possible tetrahedral environments of the $Si(0Al)_A$ and $Si(0Al)_B$ sites, as determined in this work for zeolite β, are shown in Fig. 6.

It is noteworthy that the number of Si(0Al) sites eliminated in the course of Si $\rightarrow$ Al substitution is generally greater than the number of inserted Al atoms (48). In accordance with the experimental results, an Al atom, which substitutes the central silicon, should eliminate 3 Si(0Al) sites and 1 Si(2Al) site and generate 2 Si(1Al) sites, 1 Si(2Al) site, and 1 Si(3Al) site (see $Si(0Al)_A$ site in Fig. 6). That is to say, when an Al atom substituting the central silicon of $Si(0Al)_A$ site, the Si(1Al) sites should be increased to 2. The difference in relative population of $Si(0Al)_B$ sites in Hβ(0.03) and Hβ(0) samples is 2.7 (Table 3). It is probable that the $Si(0Al)_A$ site converts to the $Si(0Al)_B$ site; i.e., 2.7 $Si(0Al)_A$ sites of the Hβ(0) sample are converted to $Si(0Al)_B$ sites during the $NaAlO_2$ solution treatment, so that 20.6 $Si(0Al)_A$ sites are present in the Hβ(0) sample. However, the Hβ(0.03) sample has only 18.6 $Si(0Al)_A$ sites, on which the relative population of $Si(0Al)_A$ sites of the Hβ(0.03) sample is smaller by 2 compared with the Hβ(0) sample. Therefore, 0.67 Al atoms substituting the central silicon eliminate 2 $Si(0Al)_A$ sites and add 1.3 Si(1Al) sites, which adds 14.4 Si(1Al) sites to Hβ(0). The total relative number of 15.7 Si(1Al) sites is approximately the same as

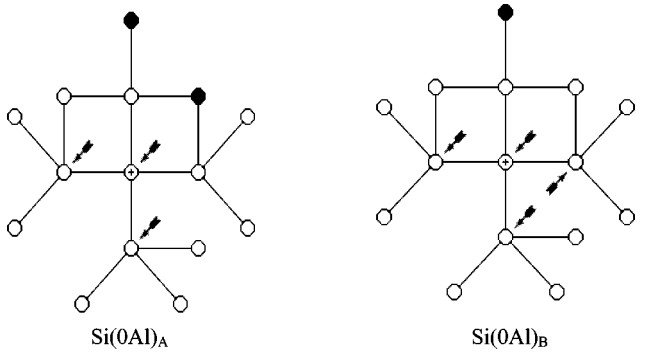

FIG. 6. Possible tetrahedral environments of a silicon atom (marked with a cross) in the zeolite β framework. Open circles, silicon; closed circles, aluminum; arrows, Si(0Al) sites.

the relative number of Si(1Al) sites in Hβ(0.03). According to this analysis, we deduce that the framework $Si(0Al)_A$ sites in zeolite β (Fig. 6) may be the main realumination sites during the treatment with an $NaAlO_2$ solution.

The actual process may be more complex. The substitution mechanism cannot be completely ignored, and further work is needed to specify it.

CONCLUSIONS

Acid sites of Hβ zeolite are related to the treatment conditions of zeolite β. When zeolite β is treated with an $NaAlO_2$ solution, its surface acid properties change in such a way that (i) the amount of strong and weak acid increases, (ii) the strength of the Brønsted sites increases to a greater extent than that of the Lewis acid sites, (iii) the number of Brønsted and Lewis acid sites increases. Therefore, for disproportionation and transalkylation of toluene and C_9 aromatics, the catalytic activity of zeolite β, treated with an $NaAlO_2$ solution, is higher than that of untreated zeolite β.

The framework $Si(0Al)_A$ sites in zeolite β may be the main realumination sites through isomorphic substitution by $Al(OH)_4^-$ anions during the $NaAlO_2$ solution treatment. In addition, the presence of two different framework tetrahedral alumina of sites A and B was proved, and the dealumination of TEA β during calcination may take place at the Si(2Al) site seen in the ^{29}Si MAS NMR spectra and at the T_dAl of site B shown in the ^{27}Al MAS NMR spectra.

REFERENCES

1. Sulikowski, B., *Heterog. Chem. Rev.* **3**, 203 (1996).
2. Sulikowski, B., Datka, J., Gil, B., Ptaszynski, P., and Klinowski, J., *J. Phys. Chem. B* **101**, 6929 (1997).
3. Sulikowski, B., Rakoczy, J., Hamdan, H., and Klinowski, J., *J. Chem. Soc., Chem. Commun.* 1542 (1987).
4. Chang, C. D., Chu, C. T.-W., Miale, J. N., Bridger, R. F., and Calvert, R. B., *J. Am. Chem. Soc.* **106**, 8143 (1984).
5. Anderson, M. W., Klinowski, J., and Liu, X., *J. Chem. Soc., Chem. Commun.* 1596 (1984).
6. Liu, X., Klinowski, J., and Thomas, J. M., *J. Chem. Soc., Chem. Commun.* 582 (1986).
7. Man, P. P., and Klinowski, J., *J. Phys. Chem. Lett.* **147**, 581 (1988).
8. Hamdan, H., and Klinowski, J., *ACS Symp. Ser.* **398**, 465 (1989).
9. Hamdan, H., Sulikowski, B., and Klinowski, J., *J. Phys. Chem.* **93**, 350 (1989).
10. Lietz, G., Schnabal, K. H., Peuker, Ch., Gross, Th., Storek, W., and Völter, J., *J. Catal.* **148**, 562 (1994).
11. Dessan, R. M., and Kerr, G. T., *Zeolites* **4**, 315 (1984).
12. Yamagishi, K., Namba, S., and Yashima, T., *J. Catal.* **121**, 47 (1990).
13. Zhang, Z., Liu, X., Xu, Y., and Xu, R., *Zeolites* **11**, 232 (1991).
14. Wadlinger, R. L., Kerr, G. T., and Rosinski, E. J., U.S. Patent 3308069, 1967.
15. Treacy, M. M. J., and Newsam, J. M., *Nature (London)* **332**, 249 (1988).
16. Boretto, L., Camblor, M. A., Corma, A., and Perez-Pariente, J., *Appl. Catal.* **82**, 37 (1992).
17. Lee, J. K., and Rhee, H. K., *Catal. Today* **38**, 235 (1997).
18. Wang, Z. B., Kamo, A., Youeda, T., Komatsu, T., and Yashima, T., *Appl. Catal.* **159**, 119 (1997).
19. Das, J., Bhat, Y. S., and Halgeri, A. B., *Catal. Lett.* **23**, 161 (1994).
20. Wang, I., Tsai, T. C., and Huang, S. T., *Ind. Eng. Chem. Res.* **29**, 2005 (1990).
21. Reddy, K. S. N., Eapen, M. J., Soni, H. S., and Shiralkar, P. V., *J. Phys. Chem.* **96**, 7923 (1992).
22. Ione, K. G., Stephanov, V. G., Echevskii, G. V., Shubin, A. A., and Paukshtis, E. A., *Zeolites* **4**, 114 (1984).
23. Sauer, J., *J. Mol. Catal.* **54**, 312 (1989).
24. Kiricsi, I., Flego, C., Pazzuconi, G., Parker, W. O., Millini, Jr., R., Perego, C., and Bellussi, G., *J. Phys. Chem.* **98**, 4627 (1994).
25. Bourgeat-Lami, E., Massiani, P., DiRenzo, F., Espiau, P., and Fajula, F., *Appl. Catal.* **72**, 139 (1991).
26. Bourgeat-Lami, E., Massiani, P., Di Renzo, F., Fajula, F., and Courieres, T. D., *Catal. Lett.* **5**, 265 (1990).
27. Maache, M., Janin, A., and Lavalley, J. C., *Zeolites* **13**, 419 (1993).
28. Borade, R. B., and Clearfield, A., *J. Phys. Chem.* **96**, 6729 (1992).
29. Perez-Pariente, J., Sanz, J., Fornes, V., and Corma, A., *J. Catal.* **124**, 217 (1990).
30. Jia, C., Mossiani, P., and Barthomeuf, D., *J. Chem. Soc., Faraday Trans.* **89** (19), 3659 (1993).
31. Yang, C., and Xu, Q. *Zeolites* **19**, 404 (1997).
32. Xie, Z. K., Chen, Q. L., Zhang, C. F., Bao, J. Q., and Cao, Y. H., *J. Phys. Chem. B* **104**, 2853 (2000).
33. Robb, G. M., Zhang, W. M., and Smirniotis, P. G., *Micropor. Mesopor. Mater.* **20**, 315 (1998).
34. Chao, K. J., Sheu, S. P., Lin. L. H., Genet, M. J., and Feng, M. H., *Zeolites* **18**, 18 (1997).
35. Massiani, P., Chauvin, B., Fajula, F., and Figueras, F., *Appl. Catal.* **42**, 105 (1988).
36. Fyfe, C. A., Strobl, H., Kokotailo, G. T., Pasztor, C. T., Barlow, G. E., and Bradley, S., *Zeolite* **8**, 132 (1988).
37. Meier, W. M., and Olson, D. H., "Atlas of Zeolite Structure Types," 3rd edition, p. 58. Butterworh-Heinemann, Oxford, UK, 1992.
38. Mostowicz, R., Testa, F., and Fonseca, A., *Zeolites* **18**, 308 (1997).
39. van Bokhoven, J. A., Koningsberger, D. C., Kunkeler, P., vanBekkum, H., and Kentgens, A. P. M., *J. Am. Chem. Soc.* **122**(51), 12,842 (2000).
40. Chauvin, B., Massiani, P., Dutartre, F. F., and Fajula , F., *Zeolites* **10**, 174 (1990).
41. Klinowski, J., and Anderson, M. W., *J. Chem. Soc., Faraday Trans.* **82**, 569 (1986).
42. Briscoe, N., Casci, J. L., Daniels, J. A., Johnson, D. W., Shannon, M. D., and Stewart, A., *Stud. Surf. Sci. Catal. A* **49**, 151 (1989).
43. Beaumont, R., and Barthomeuf, D., *J. Catal.* **26**, 218 (1972).
44. van Hooff, J. H. C., and Rolofsen, J. W., *Stud. Surf. Sci. Catal.* **58**, 241 (1991).
45. Kosslick, H., Tuan, V. A., Frivke, R., and Martin, A., *Stud. Surf. Sci. Catal.* **84**, 1013 (1994).
46. Beyer, H. K., Brobely-Plane, G., and Wu, J., *Stud. Surf. Sci. Catal.* **84**, 933 (1994).
47. Apelian, M. R., Fung, A. S., Kennedy, G. J., and Degnan, T. F., *J. Phys. Chem.* **100**, 16577 (1996).
48. Klinowski, J., *Stud. Surf. Sci. Catal.* **52**, 39 (1989).
49. Guisnet, M., Ayrault, P., and Datka, J., *Micropor. Mesopor. Mater.* **20**, 283 (1998).
50. Jian, Q. Z., Jing, D. Z., Ma, J., and Guo, J. F., *Acta Sientiarum Naturalium Universitalis*, Jilinnensis **4**, 107 (1993).
51. Gao, T. N., Jia, T. W., and Wang, J. Z., *Acta Petroli Sinica* (Petroleum Processing Section) **10**, 36 (1994).
52. Wu, P., Komatsu, T., and Yashima, T., *J. Phys. Chem.* **99**, 10923 (1995).
53. Yamagishi, K., Namba, S., and Yashima, T., *J. Phys. Chem.* **95**, 872 (1991).
54. Yang, C., and Xu, Q. H., *J. Chem. Soc., Faraday Trans.* **93**(8), 1675 (1997).
55. Loewenstein, W., *Mineral Am.* **39**, 92 (1953).